
Improved Mixed-Example Data Augmentation

Cecilia Summers

Department of Computer Science
University of Auckland
cecilia.summers.07@gmail.com

Michael J. Dinneen

Department of Computer Science
University of Auckland
mjd@cs.auckland.ac.nz

Abstract

In order to reduce overfitting, neural networks are typically trained with data augmentation, the practice of artificially generating additional training data via label-preserving transformations of existing training examples. Recent work has demonstrated a surprisingly effective type of non-label-preserving data augmentation, in which pairs of training examples are averaged together. In this work, we generalize this “mixed-example data augmentation”, which allows us to find methods that improve upon previous work. This generalization also reveals that linearity is not necessary as an inductive bias in order for mixed-example data augmentation to be effective, providing evidence against the primary theoretical hypothesis from prior work.

1 Introduction

Deep neural networks have demonstrated remarkable performance on many tasks previously considered intractable, but they come with a cost: they require large amounts of data. While great progress has been made at making neural nets more data-efficient through the use of improved network architectures and training methods, the limitation of data remains.

To get around the requirement for large amounts of data, machine learning practitioners typically either transfer knowledge from other tasks, or employ large amounts of “data augmentation”, the practice of generating synthetic data based on real examples. This synthetic data is used to artificially expand the size of datasets used to train neural networks, and typically takes the form of transformations that maintain the realistic appearance of the input, *e.g.* for image classification, flipping an image horizontally or making minor adjustments to its brightness.

A handful of recent work, however, has pointed out a new direction: data augmentation can take the form of combining training examples together, specifically via random linear (convex) combinations [17, 16, 8]. Though this type of data augmentation does not produce realistic-looking data, it is surprisingly effective, significantly improving performance of models across a variety of domains even *after* other forms of data augmentation. We currently do not have a good understanding of why this approach is effective; the best hypothesis comes from Zhang et al. [17], who suggest that the added linearity this form of data augmentation encourages is a useful inductive bias. Regardless, these works point to new directions for reducing the dependence of modern deep neural networks on large quantities of labeled data.

In this paper, we explore this new area of data augmentation via combining multiple examples (“mixed-example data augmentation”). We propose a variety of alternative methods for example generation, surprisingly finding that most methods result in model improvements, and even find two methods that improve upon existing work [17]. Our experiments demonstrate that the usefulness of mixed-example data augmentation is not determined by a linear inductive bias, though it may still be independently useful.

The remainder of this paper is organized as follows: In Sec. 2 we review related work in data augmentation and regularization more generally, and in Sec. 3 we present our exploration of mixed-example data augmentation, overviewing 13 alternatives. We present experiments on CIFAR-10 and CIFAR-100 in Sec. 4, then conclude with a discussion in Sec. 5.

2 Related Work

Data Augmentation. Data augmentation is key to the success of many modern neural network approaches across numerous domains. Here we focus our discussion on data augmentation as applied to images. Common forms of data augmentation include random crops, horizontal flipping, and color augmentation [11], which improve robustness to translation, reflection, and illumination. Occasionally random scalings are also done [14], as well as random rotations and affine transformations, though these tend to get less use. One more recent form of data augmentation consists of zeroing out random parts of the image [3, 18], which works surprisingly well on the CIFAR-10/100 datasets. All of these methods are a form of label-preserving data augmentation, *i.e.* they are designed to maintain the label of the transformed image, which requires a small amount of task-specific knowledge. For example, in the context of image classification, an image of a cat, after any of these types of data augmentation, is still recognizable as an image of a cat.

More directly relevant to our work is recent progress on generating images for training as linear combinations of other training images [17, 16, 8]. Of these, *mixup* [17] is perhaps the most general, and consists of generating a random mixing parameter $\lambda \sim \text{Beta}(\alpha, \alpha)$ and producing a new image and label as a convex combination of two images/labels, with weight λ . Building upon this, our work considers more general functions that combine information from multiple examples.

Regularization. Closely related to the topic of data augmentation is regularization. One of the most common approaches to regularization is *weight decay* [12], which is equivalent to L_2 -regularization when using a vanilla stochastic gradient descent learning rule. Other common types of regularization include Dropout [15], which can also be considered a form of data augmentation injected at intermediate layers in a neural network, and Batch Normalization [9], which has a regularization effect due to randomness in minibatch statistics. Other more exotic forms of regularization include randomly dropping out layers [7] and introducing disconnects between forward- and backward-propagation [4]. It is folk wisdom that there is a tradeoff between the amount of data augmentation and the optimal amount of regularization to use — for example, Zhang et al. [17] found that using *mixup* well required a 5x lower amount of weight decay than without *mixup* on CIFAR-10.

3 Methods

In *mixup* [17], arguably the most generalized version of [17, 16, 8], a new training example and label (\tilde{x}, \tilde{y}) is created from two input training examples $(x_i, y_i), (x_j, y_j)$ as

$$\begin{aligned}\tilde{x} &= \lambda x_i + (1 - \lambda)x_j \\ \tilde{y} &= \lambda y_i + (1 - \lambda)y_j\end{aligned}\tag{1}$$

where $\lambda \sim \text{Beta}(\alpha, \alpha)$ for each pair of examples, with α a hyperparameter. For experiments on CIFAR-10 and CIFAR-100, Zhang et al. [17] used the value $\alpha = 1$, which results in a uniform distribution between 0 and 1. *Mixup* is motivated as encouraging linearity between training examples, and that such linearity is an effective inductive bias (an assumption built into a model) for most models, and was previously demonstrated to be useful across a wide variety of tasks and models. In this work, we instead focus on the view that mixed-example generation of novel training data is useful in general as a form of data augmentation and regularization. Indeed, we have found that the improved performance *mixup* and other related methods has had can be obtained by extremely non-linear forms of mixed-example data augmentation.

We seek to expand the set of functions considered to arbitrary functions of the form:

$$(\tilde{x}, \tilde{y}) = f(\{(x_i, y_i)\}_{i=1}^2)\tag{2}$$

i.e. arbitrary functions mapping two examples into a single new training example, which subsumes the linear combinations used in previous work. We note that one can in theory consider functions with $N > 2$ examples as input, but in initial experiments (and agreeing with [17]) we did not see improvement beyond $N = 2$, so we restrict our methods to this setting.

We now illustrate the generality of this formulation by presenting many different methods for mixed-example data augmentation. We note that most of these methods are orthogonal to approaches such as *mixup* or other more traditional forms of data augmentation and can potentially be employed in combination with them. Illustrative examples are shown in Fig. 1.

Noisy Mixup. Normally, in *mixup* [17], a single $\lambda \sim \text{Beta}(\alpha, \alpha)$ is sampled and then used across the entire image. However, in order to produce an output with an expected label of $\lambda y_i + (1 - \lambda)y_j$, there is no need for λ to be the same across an entire image – instead, as long as its expectation is the same, the same label applies. In this method, we first sample λ in the same fashion, but then for each pixel identified by a row r and column c we add random zero-centered noise to the mixing coefficient: $\lambda_{r,c} = \lambda + \ell_{r,c}$ where $\ell_{r,c} \sim N(0, \sigma^2)$, with σ^2 a hyperparameter.

Vertical Concat. As before, sample $\lambda \sim \text{Beta}(\alpha, \alpha)$. However, in this method we vertically concatenate the top λ fraction of image x_i with the bottom $(1 - \lambda)$ fraction of image x_j , which is a non-linear transformation with respect to the input. The label \tilde{y} remains equal to $\lambda y_i + (1 - \lambda)y_j$.

Horizontal Concat. Similar to vertical concat, horizontally concatenate the left λ fraction of image x_i with the right $(1 - \lambda)$ fraction of image x_j .

Mixed Concat. This is a combination of vertical and horizontal concatenation: first we sample $\lambda_1, \lambda_2 \sim \text{Beta}(\alpha, \alpha)$. Then, divide the output image in a 2×2 grid as shown in Fig. 1, where the horizontal boundary between grid members is determined by λ_1 and the vertical boundary is determined by λ_2 . Assign the top-left and bottom-right to x_i and the top-right and bottom-left to x_j , with $\tilde{y} = (\lambda_1 \lambda_2 + (1 - \lambda_1)(1 - \lambda_2))y_i + (\lambda_1(1 - \lambda_2) + (1 - \lambda_1)\lambda_2)y_j$, *i.e.* \tilde{y} is determined by the relative area of x_i vs x_j .

Random 2×2 . Similarly to “Mixed Concat.”, this method divides the image into a 2×2 grid with random sizes as before, but instead of using a fixed assignment of grid cells to input images, randomly decides for each square in the grid whether it should take content from x_i or x_j . As before, \tilde{y} is measured as a function of the relative area of x_i vs x_j .

VH-Mixup. First, two intermediate images are made as the result of “Vertical Concat.” and “Horizontal Concat.”, each with their own randomly chosen λ . Then, *mixup* is applied with these two images as input. This produces an image where the top-left is from x_i , the bottom-right is from x_j , and the top-right and bottom-left are mixed between the two, with difference mixing coefficients. The label \tilde{y} is determined in a straightforward manner based on the rules for label generation in “Vertical Concat.”, “Horizontal Concat.”, and *mixup*.

Random Square. With image x_i as the base, a random square within the image is replaced with a portion of x_j . This method is inspired by Cutout [3] and random erasing data augmentation [18], but instead of replacing the subimage with 0, we replace it with part of a different image. As in Cutout, the size of the square is a hyperparameter, which we set to 16 pixels.

Random Column Interval. This is a slight generalization of “Horizontal Concat.” — a random interval of columns is picked and that part of image x_i is replaced with columns in x_j . The difference between this method and “Horizontal Concat.” is that this column interval need not begin with the first column. The interval in this method is picked by sampling the lower bound of the interval uniformly, with the upper bound then sampled uniformly between all possible remaining upper bounds.

Random Row Interval. This method is identical to “Random Column Interval” but is applied to a random interval of rows instead of columns.

Random Rows. For each row in the output image \tilde{x} , this method randomly samples whether to take the row from x_i or x_j , where the probability of choosing the corresponding row in x_i is given by

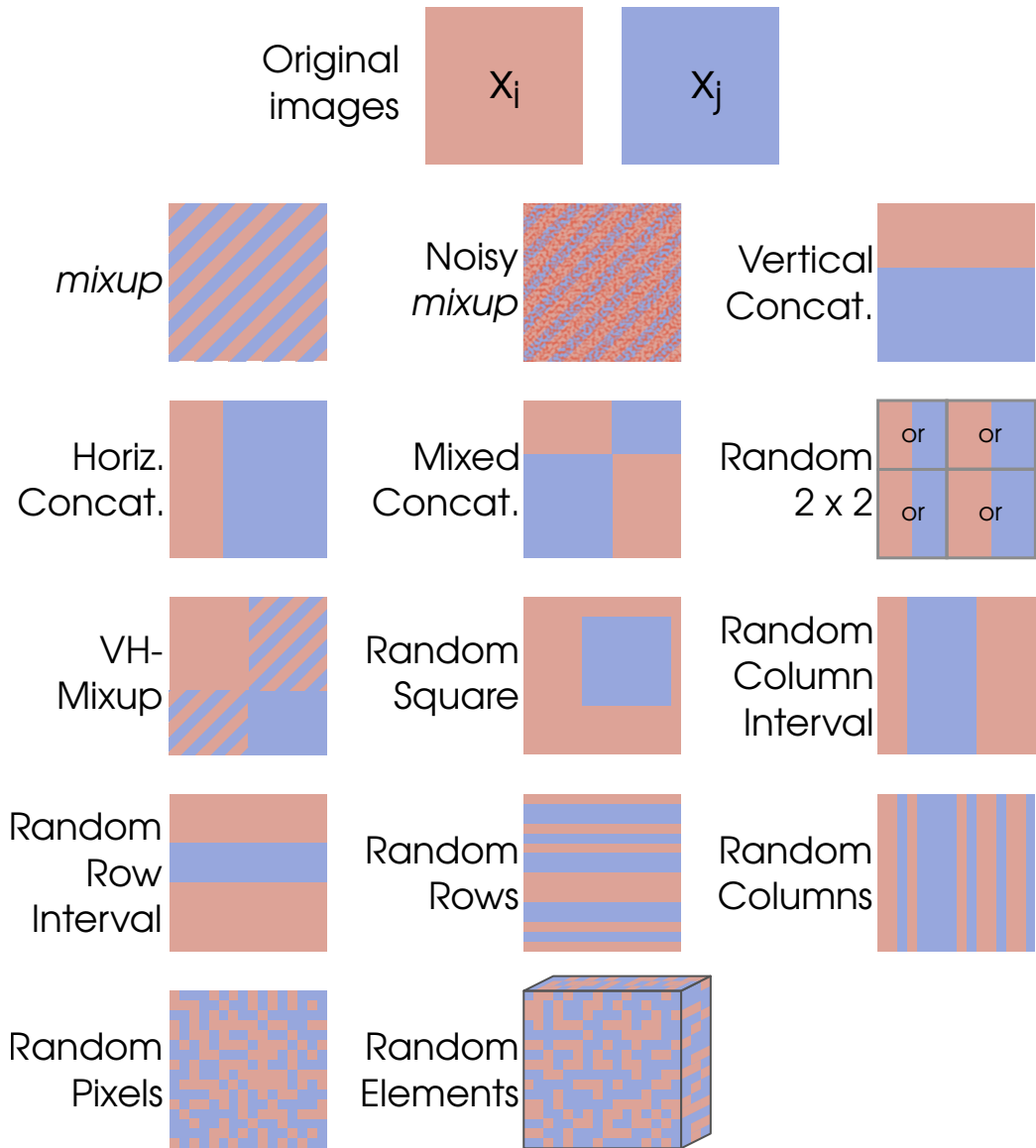


Figure 1: Example outputs for each mixed-example data augmentation method. See text (Sec. 3) for details of each method. Diagonal stripes are used to indicate element-wise weighted averaging. Note that for “VH-Mixup”, the bottom-left and upper-right region used potentially different weights for the weighted average.

λ . As before, \tilde{y} is determined based on the fraction of rows that were taken from x_i compared with x_j .

Random Columns. This method is identical to “Random Rows” but samples columns instead of rows.

Random Pixels. This method is identical to “Random Rows” but samples each pixel separately.

Random Elements. This method is identical to “Random Rows” but samples each element of the image separately. That is, when the image is represented as a $\text{Height} \times \text{Width} \times 3$ tensor (represented in RGB), each element in the tensor is randomly sampled from the corresponding value in either x_i or x_j .

Table 1: Experimental results on CIFAR-10 and CIFAR-100. All numbers are the average accuracy across three training runs, measured at the final step of training, and methods are ordered by performance. Numbers for the baseline ResNet-18 model and *mixup* are from our TensorFlow re-implementation.

	Method	Error (%)		Method	Error (%)
	CIFAR-10	ResNet-18		5.4	CIFAR-100
<i>mixup</i> [17]		4.3	<i>mixup</i> [17]	22.4	
Rand. Elems.		6.2	Rand. Elems.	26.5	
Rand. Pixels		5.7	Rand. Pixels	26.0	
Rand. Row. Int.		5.3	Rand. Col. Int.	25.3	
Rand. Col. Int.		5.1	Rand. Cols	24.1	
Rand. Cols		4.8	Noisy Mixup	23.3	
Horiz. Concat.		4.7	Rand. Row. Int.	23.2	
Rand. Rows		4.6	Horiz. Concat.	23.1	
Noisy Mixup		4.5	Rand. Square.	22.9	
Vert. Concat.		4.4	Rand. Rows	22.8	
Mixed. Concat.		4.4	Vert. Concat.	21.4	
Rand. Square.		4.3	Mixed. Concat.	21.4	
Rand. 2×2		4.1	Rand. 2×2	21.4	
VH-Mixup		3.8	VH-Mixup	20.5	

4 Experiments

4.1 Implementation Details

Following [17], we do most of our experiments with the pre-activation ResNet-18 [5], which we re-implemented in TensorFlow [1]. We note that this variant is slightly different from the official ResNet-18, attaining higher accuracy. As in [17], we use $\alpha = 1$ where applicable and use a weight decay of 10^{-4} (or $5 \cdot 10^{-4}$ for the baseline ResNet-18). Following [5], we use minibatches of size 128, the learning rate starts at .01 for a warm-up period, going up to 0.1 at 400 steps, then decays by a factor of 10 after 32000, 48000, and 70000 steps. In practice, we noticed that this learning rate strategy can be somewhat unstable, with losses spiking up at the 400-step transition, after which models fail to recover well and end up with a few percent lower accuracy than they would otherwise. Therefore, we have taken the practice of running models for three epochs (≈ 1200 steps) and only continuing them when such a spike is not observed.

Unlike [17], we perform our data augmentation by directly pairing examples together, rather than doing it on a batch-by-batch basis. While this could potentially slow down data processing, it is somewhat simpler to develop with, especially for the more complicated data generation methods, and we found that we were still able to generate data fast enough for models to use. Initial experiments furthermore suggested that this does not affect accuracy. We also found that it was crucial to do other types of data augmentation (*i.e.* random cropping and flips) before applying any type of mixed-example data augmentation, with differences in accuracy greater than 1%, but do not currently have an explanation for why this is important. All experiments were done using two Nvidia Geforce GTX 1080 Ti GPUs.

4.2 CIFAR-10

CIFAR-10 [10] consists of 60,000 images of size 32×32 pixels, split evenly among 10 categories, with 50,000 training images and 10,000 test images, and is a standard test-bed for training of small-scale deep learning models. Results on CIFAR-10 are shown in Table 1 (left). A few trends are immediately apparent:

First, with the exception of “Rand. Pixels” and “Rand. Elems”, all other mixed-example techniques do, in fact, improve upon the baseline ResNet which uses only standard data augmentation. This illustrates that the space of effective mixed-example data augmentation is much larger than realized in previous work [17, 16, 8]. Even the simplest of methods, “Horiz. Concat” and “Vert Concat”, improved upon the baseline significantly, and are perhaps the least similar to prior work of the methods considered.

We also observe that no linearity at all is required in order to be extremely effective. “Rand. 2×2 ”, despite containing no element-wise weighted averaging, is just as useful a form of data augmentation as *mixup* and related methods, even slightly outperforming it the sample set of runs we conducted. While previous work has shown that using linearity as an inductive bias on its own can be fruitful, it is by no means necessary.

However, by combining the insights of linearity as an inductive bias with the alternative types of mixed-example data augmentation, we were able to produce a method (“VH-Mixup”) that was able to outperform either approach on its own, setting a new state of the art for mixed-example data augmentation. This result is particularly promising due to the nascency of mixed-example approaches and the general applicability to a wide range of tasks (for the methods in this paper, tasks in computer vision).

Last, it is worth remarking on the methods that did *not* work as well. In particular, “Rand. Elems” and “Rand. Pixels” both worked worse than the baseline of doing no mixed-example data augmentation. These methods have something in common: the tendency to introduce high-frequency signals in the data. We hypothesize that this type of data augmentation makes it somewhat more difficult for models to capture local details within images, forcing them to rely more on low-frequency content. We also note that “Noisy Mixup”, although it worked reasonably well, was not as effective as regular *mixup*, which we also attribute to the addition of high-frequency content.

4.3 CIFAR-100

CIFAR-100 [10] is a 100-class companion of CIFAR-10 with otherwise identical properties. We present our results on CIFAR-100 in Table 1 (right). Trends here are largely similar to results on CIFAR-10, with the best and worst methods consistent, though the ordering in between changes somewhat. We note that we had more trouble reproducing prior work on CIFAR-100, with our baseline pre-activation ResNet-18 2.0% better than previously reported, and our *mixup* implementation 1.3% worse than previously. We believe that this difference is likely due to some combination of subtle implementation detail differences between the original PyTorch implementation and our TensorFlow re-implementation, along with potentially different hyperparameter settings — in some initial experiments, we were able to improve the performance of our *mixup* implementation by 0.9% on CIFAR-100 by using a different weight decay, which also improved VH-Mixup by 0.7%. To keep all methods on a level playing field, though, we have kept a constant weight decay of 10^{-4} across all mixed-example data augmentation methods.

5 Discussion

In this paper we have proposed several variants of mixed-example data augmentation, generalizing and improving upon recent work [17, 16, 8]. Our methods, while specific to image-based tasks, are straightforward to implement and reveal a surprisingly large spectrum for what effective mixed-example data augmentation can look like. Though we considered a variety of methods in this work, it is likely that even more effective methods exist, and we hope that our explorations help inspire further research in the area.

Key questions for future research include developing an understanding for *why* mixed-example data augmentation works and determining which specific properties of such augmentation methods are useful. Previous work [17] hypothesized that the key property enabling its effectiveness is the establishment of linearity as an inductive bias. In this work we have shown that, while linearity may be helpful, it is by no means necessary, and there exist methods without any linearity that are competitive with or even better than strictly linear methods. On a lower level, it would also be interesting to understand the relationship between mixed-example data augmentation and other more traditional forms of data augmentation. For example, we have found the puzzling behavior that mixed-example data augmentation is only effective when performed after other forms of data augmentation, a detail which is also shared by all open-source implementations of related work we have found.

One disadvantage of our approach is that, unlike prior work [17, 16, 8], our methods operate only on images. While this is true, we believe it is likely that domain-specific approaches such as ours can be made for other problems, such as speech [6] or natural language processing [2]. Furthermore, we believe that such approaches hold the most promise for data-starved tasks such as robotics [13].

References

- [1] Martín Abadi, Paul Barham, Jianmin Chen, Zhifeng Chen, Andy Davis, Jeffrey Dean, Matthieu Devin, Sanjay Ghemawat, Geoffrey Irving, Michael Isard, et al. Tensorflow: A system for large-scale machine learning. In *OSDI*, volume 16, pages 265–283, 2016.
- [2] Ronan Collobert, Jason Weston, Léon Bottou, Michael Karlen, Koray Kavukcuoglu, and Pavel Kuksa. Natural language processing (almost) from scratch. *Journal of Machine Learning Research*, 12(Aug):2493–2537, 2011.
- [3] Terrance DeVries and Graham W Taylor. Improved regularization of convolutional neural networks with cutout. *arXiv preprint arXiv:1708.04552*, 2017.
- [4] Xavier Gastaldi. Shake-shake regularization. *arXiv preprint arXiv:1705.07485*, 2017.
- [5] Kaiming He, Xiangyu Zhang, Shaoqing Ren, and Jian Sun. Identity mappings in deep residual networks. In *European Conference on Computer Vision*, pages 630–645. Springer, 2016.
- [6] Geoffrey Hinton, Li Deng, Dong Yu, George E Dahl, Abdel-rahman Mohamed, Navdeep Jaitly, Andrew Senior, Vincent Vanhoucke, Patrick Nguyen, Tara N Sainath, et al. Deep neural networks for acoustic modeling in speech recognition: The shared views of four research groups. *IEEE Signal Processing Magazine*, 29(6):82–97, 2012.
- [7] Gao Huang, Yu Sun, Zhuang Liu, Daniel Sedra, and Kilian Q Weinberger. Deep networks with stochastic depth. In *European Conference on Computer Vision*, pages 646–661. Springer, 2016.
- [8] Hiroshi Inoue. Data augmentation by pairing samples for images classification. *arXiv preprint arXiv:1801.02929*, 2018.
- [9] Sergey Ioffe and Christian Szegedy. Batch normalization: Accelerating deep network training by reducing internal covariate shift. *arXiv preprint arXiv:1502.03167*, 2015.
- [10] Alex Krizhevsky and Geoffrey Hinton. Learning multiple layers of features from tiny images. 2009.
- [11] Alex Krizhevsky, Ilya Sutskever, and Geoffrey E Hinton. Imagenet classification with deep convolutional neural networks. In *Advances in neural information processing systems*, pages 1097–1105, 2012.
- [12] Anders Krogh and John A Hertz. A simple weight decay can improve generalization. In *Advances in neural information processing systems*, pages 950–957, 1992.
- [13] Sergey Levine, Chelsea Finn, Trevor Darrell, and Pieter Abbeel. End-to-end training of deep visuomotor policies. *The Journal of Machine Learning Research*, 17(1):1334–1373, 2016.
- [14] Karen Simonyan and Andrew Zisserman. Very deep convolutional networks for large-scale image recognition. *ICLR*, 2015.
- [15] Nitish Srivastava, Geoffrey Hinton, Alex Krizhevsky, Ilya Sutskever, and Ruslan Salakhutdinov. Dropout: A simple way to prevent neural networks from overfitting. *The Journal of Machine Learning Research*, 15(1):1929–1958, 2014.
- [16] Yuji Tokozume, Yoshitaka Ushiku, and Tatsuya Harada. Between-class learning for image classification. *arXiv preprint arXiv:1711.10284*, 2017.
- [17] Hongyi Zhang, Moustapha Cisse, Yann N Dauphin, and David Lopez-Paz. mixup: Beyond empirical risk minimization. *ICLR*, 2018.
- [18] Zhun Zhong, Liang Zheng, Guoliang Kang, Shaozi Li, and Yi Yang. Random erasing data augmentation. *arXiv preprint arXiv:1708.04896*, 2017.